ELSEVIER

Physics of the Earth and Planetary Interiors 132 (2002) 157–175

PHYSICS OF THE EARTH AND PLANETARY INTERIORS

www.elsevier.com/locate/pepi

Slab-pull and slab-push earthquakes in the Mexican, Chilean and Peruvian subduction zones

A. Lemoine[a,*], R. Madariaga[a], J. Campos[b]

[a] *Laboratoire de Géologie, Ecole Normale Supérieure, 24 Rue Lhomond, 75231 Paris Cedex 05, France*
[b] *Departamento de Geofísica, Universidad de Chile, Santiago, Chile*

Abstract

We studied intermediate depth earthquakes in the Chile, Peru and Mexican subduction zones, paying special attention to slab-push (down-dip compression) and slab-pull (down-dip extension) mechanisms. Although, slab-push events are relatively rare in comparison with slab-pull earthquakes, quite a few have occurred recently. In Peru, a couple slab-push events occurred in 1991 and one slab-pull together with several slab-push events occurred in 1970 near Chimbote. In Mexico, several slab-push and slab-pull events occurred near Zihuatanejo below the fault zone of the 1985 Michoacan event. In central Chile, a large $M = 7.1$ slab-push event occurred in October 1997 that followed a series of four shallow $M_w > 6$ thrust earthquakes on the plate interface. We used teleseismic body waveform inversion of a number of $M_w > 5.9$ slab-push and slab-pull earthquakes in order to obtain accurate mechanisms, depths and source time functions. We used a master event method in order to get relative locations. We discussed the occurrence of the relatively rare slab-push events in the three subduction zones. Were they due to the geometry of the subduction that produces flexure inside the downgoing slab, or were they produced by stress transfer during the earthquake cycle? Stress transfer can not explain the occurence of several compressional and extensional intraplate intermediate depth earthquakes in central Chile, central Mexico and central Peru. It seemed that the heterogeneity of the stress field produced by complex slab geometry has an important influence on intraplate intermediate depth earthquakes.

Keywords: Subduction; Intermediate depth intraplate earthquakes; Nazca plate; Cocos plate; Flat subduction; Plate flexure

1. Introduction

We studied intermediate depth earthquakes which occured inside the downgoing subducted plate in the Eastern Pacific subduction zones from Chile to Mexico. This kind of event is often more destructive than the typical interplate subduction events because hypocenters are usually inland, below large population centers. For example, in Southern Chile, the large $M_w = 7.8$ normal fault, intermediate depth Chillán earthquake (Lomnitz, 1971; Kelleher, 1972) on 24 January 1939 caused close to 30.000 fatalities.

Intraplate intermediate depth earthquakes have been studied by a number of authors (Malgrange et al., 1981; Malgrange and Madariaga, 1983; Singh et al., 1985, 1999, 2000; Astiz and Kanamori, 1986; Astiz, 1987; Astiz et al., 1988; Lay et al., 1989; Cocco et al., 1997). They occur in the subducted plate, at some distance down-dip from the strongly coupled interplate interface.The fault plane commonly chosen is the most nearly vertical one (Cocco et al., 1997; Mikumo et al., 1999; Hernandez et al., 2001). Several of these authors have suggested a temporal relationship between large intraplate earthquakes at intermediate depth, outer rise

* Corresponding author.
E-mail address: lemoine@geologie.ens.fr (A. Lemoine).

0031-9201/02/$ – see front matter © 2002 Elsevier Science B.V. All rights reserved.
PII: S0031-9201(02)00050-X

earthquakes and large shallow thrust events in coupled subduction zones (Christensen and Ruff, 1983; Astiz and Kanamori, 1986; Astiz, 1987; Astiz et al., 1988; Dmowska et al., 1988; Christensen and Ruff, 1988; Dmowska et al., 1996; Taylor et al., 1996, 1998). They suggested that before a large thrust event, the interface between the downgoing and the overriding plates is strongly coupled so that the subducted slab is under tensional stresses at intermediate depth due to slab-pull. After the occurrence of a large interplate thrust earthquake, on the other hand, the slab would be under compressional stresses due to stress relaxation at the plate interface. Dmowska et al. (1988, 1996), Taylor et al. (1996, 1998) modeled this stress transfer during the earthquake cycle in coupled subduction zones. Their results are compatible with the general idea that down-dip extensional and compressional events should occur before and after shallow interplate thrust events, respectively.

Gardi et al. (2000) used a vertical 2D finite element method to simulate the subduction of the Cocos plate beneath the North American plate in central Mexico. Their results showed that the stress pattern is very sensitive to the geometry of the plate interface which is complex in this area. They showed that after a large interplate thrust earthquake associated with partial stress drop, a wide area with extensional stress remains below the down-dip edge of the fault plane of the large subduction event for a downgoing slab undergoing bending and unbending. So, the complexity of the geometry of the subducted plate could explain the occurrence of some normal faulting events at the beginning of the earthquake cycle as for example the Peruvian $M_s = 7.8$ intraplate event of 31 May 1970 which took place after the $M_s = 7.5$ shallow interplate event of 17 October 1966 (Abe, 1972; Stauder, 1975; Dewey and Spence, 1979; Beck and Ruff, 1989; Dorbath et al., 1990). Singh et al. (1985) studied the Oaxaca $M = 7.8$ intraplate normal faulting event of 15 January 1931 which occurred landward, inside the subducted Cocos plate and followed a series of large thrust earthquakes in 1928. They suggested that such events may have a role in the decoupling between the Cocos plate and the upper part of the slab and, perhaps, between the downgoing slab and the overriding continental plate. Some intermediate depth, normal faulting events occured closer to the coast under the plate interface as for example in Mexico, the events of 11 January 1997 in Guerrero ($M_w = 7.1$) (Mikumo et al., 2000) and 30 September 1999 in Oaxaca ($M_w = 7.5$) (Singh et al., 2000). Mikumo et al. (1999) explained the occurrence of the 11 January 1997 Guerrero event by its location on the zone of maximum coseismic stress increase produced by the Michoacan thrust earthquakes of 19 and 21 September 1985 ($M_s = 8.1$ and 7.6, respectively).

We studied several recent intraplate intermediate depth earthquakes in central Mexico, north central Chile and central Peru. Subduction zones beneath northern and central Peru and beneath north central Chile are characterized by a shallow dipping subducting slab, and complex geometry of the plate interface between the downgoing slab and the overriding continental plate associated with three inflection points (Stauder, 1973, 1975; Barazangi and Isacks, 1976, 1979; Isacks and Barazangi, 1977; Suárez et al., 1990; Araujo and Suárez, 1994; Gutscher et al., 2000). Subduction geometry under central Mexico is not as clear. Suárez et al. (1990), Singh et al. (1993), Pardo and Suárez (1995) found a subhorizontal geometry of the subducted Cocos plate whereas Cordoba et al. (1993), Váldes-Gonzalez and Meyer (1996), González et al. (1997) disagree with this hypothesis. There are two types of source mechanisms for intraplate intermediate depth earthquakes: slab-push and slab-pull which are associated with downplate compression and extension, respectively. If slab-pull events are relatively common in Mexico, Peru and Chile, slab-push earthquakes are very rare. We found some recent slab-push events, such as the 15 October 1997 $M_w = 7.1$ Punitaqui earthquake in north central Chile, three events in the Guerrero region in Mexico (10 December 1994, 21 June 1999 and 29 December 1999) and two events in central Peru (5 and 29 April 1991). Our goal is to describe the occurrence of such down-dip compressional and down-dip extensional events. We used teleseismic body waveform inversions in order to estimate source parameters and depth. We then use relative locations in central Mexico and north central Chile to determine the intermediate depth seismicity pattern.

2. Data analysis

2.1. Body wave data analysis

We conducted a systematic search of the harvard centroid moment tensor (CMT) database (Dziewonski

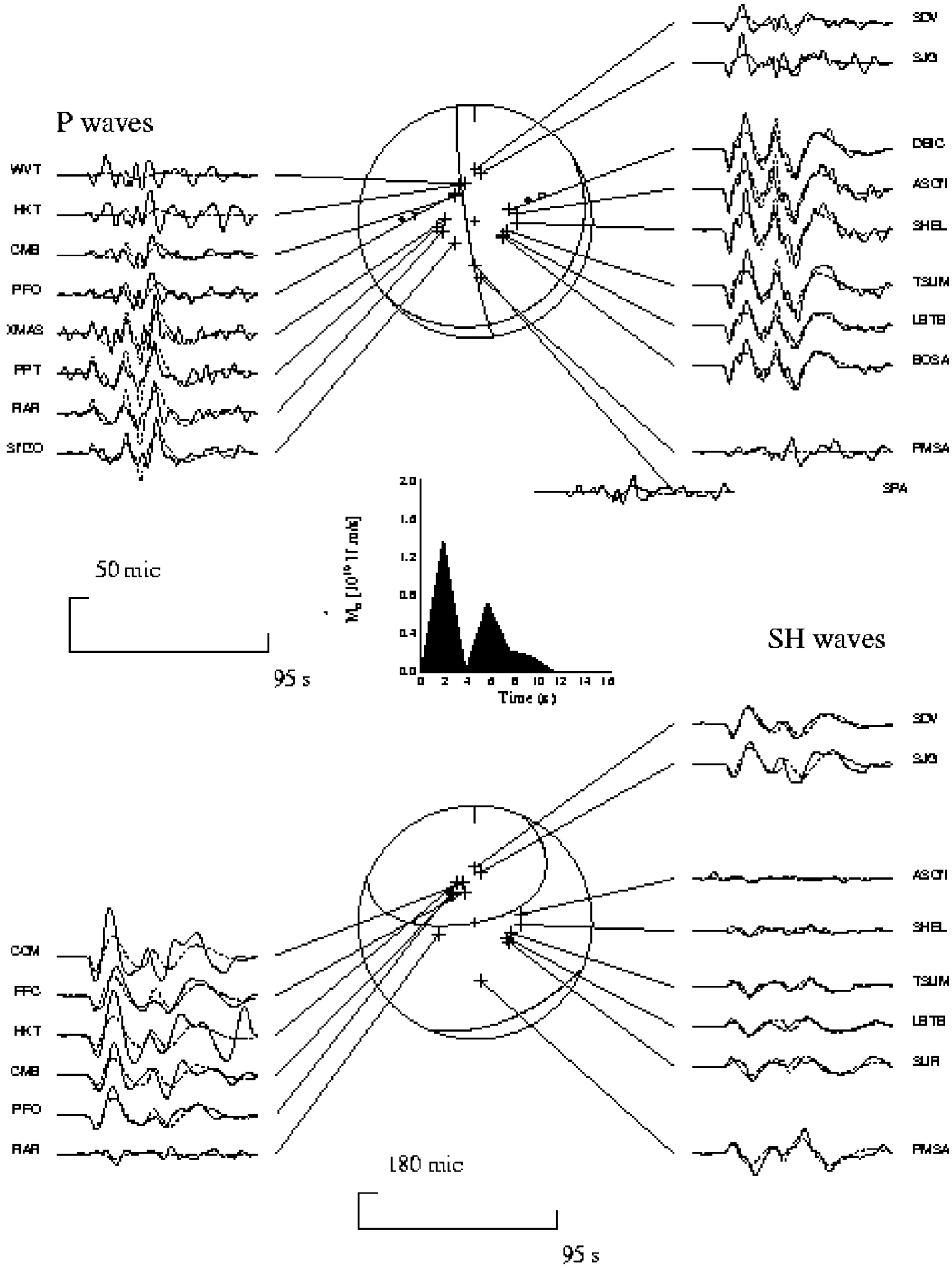

Fig. 1. Point source modelling of P- and SH-waveforms of the $M_w = 7.1$ 15 October 1997 Punitaqui earthquake in north central Chile. Its depth was 68 km. Solid and dashed lines denote observed and synthetic displacement seismograms, respectively. The overall fit is good except for P-waves at some nodal stations (WVT, HKT). Comparing the SH waveforms at stations SDV and CCM or HKT, we noticed a possible downward directivity effect on the subvertical fault. The source time function shown at the center of the figure has two main pulses of moment release. This event occured inside the downgoing Nazca plate at intermediate depth. It was a slab-oriented compressional event (slab-push).

et al., 2001) for $M_w > 6$ intermediate depth earthquakes that took place in the subduction zones of central Mexico, north central Chile and central Peru. We only looked for recent events for which a large number of digital broadband seismograms are available. We finally determined the source parameters of 16 $M_w > 5.9$ earthquakes from the inversion of far field body waveforms using all available broadband digital data recorded by global networks (IRIS and GEOSCOPE). Fig. 1 represents an example of a body waveform inversion performed for a Chilean earthquake. In order to avoid multipathing, upper mantle and core arrivals, we only inverted body waveforms from stations in the range $30^\circ < \Delta < 90^\circ$.

We modeled the earthquakes as single point double-couple sources. The velocity structure near the source and beneath the stations was approximated by a half space with standard upper mantle wave speeds. The main contributions to the seismograms come from the direct waves (P and S) and the reflected phases from the free surface (pP, sP, sS, pS). We assumed $t^* = 1$ s for P-waves and 4 s for SH-waves in order to simulate seismic attenuation. We used a maximum likelihood principle to obtain the source parameters that provide the best fit between observed and synthetic waveforms (Nábělek, 1984, 1985). In the inversion, we solved simultaneously for focal mechanism and source time function using the CMT solutions as a priori models. We selected a set of teleseismic stations that gave us the best azimuthal coverage as possible in order to have a good constraint on the fault plane parameters. We sometimes had to cope with the lack of data in the western direction which corresponds to the Pacific, because for moderate-size events it was sometimes impossible to use the noisy records from stations located on Pacific islands. We assigned weights to stations on the basis of focal sphere coverage and average amplitude of P- and SH-waves in order to reduce the possibility of a bias in the solution because of an imbalance in the data coverage. We used displacement seismograms from which the station's instrument response was deconvolved, followed by reconvolution by a common instrumental response. To avoid problems with low-and-high frequency noise, we band-passed filtered the displacement records with a band-pass Butterworth filter of order 3. The corner frequency we applied depended on the earthquakes we studied. Finally, all data were decimated to 0.5 s sample intervals.

2.2. Depth determination

The aim of our study is to try to understand the occurrence of intraplate earthquakes which took place in three different subduction zones. In order to obtain source locations inside the downgoing slab, we determined separately the source depth and epicenter. Source depth was determined using body waveforms inversion. We inverted body waveforms for a set of depths after fixing the fault mechanism. For each inversion, we calculated a normalized rms, and the best centroïd depth was taken as that which gave the lowest rms residual between observed and synthetic seismograms (Fig. 2). It is important to remark that there is always a trade-off between depth and source time function: an incorrect depth can often be compensated by changes in the source time function, producing the same synthetic seismograms (Christensen and Ruff, 1985). So, once we found a depth, we inverted the body waveforms once again, varying the other source parameters in order to obtain the best source time function associated with that particular depth. This procedure is a trial-and-error method in order to minimize the trade-off between depth and source-time function (Fig. 3).

2.3. Relative hypocenter location

In order to improve source locations, we relocated the events using the master event technique. Locations of "slave events" were determined with respect to the location of a "master event". We used a sufficiently large " master event" and assumed that it was well located by NEIC. The relative epicenter determination technique we used is based on the arrival-time differences of P-waves (Fitch, 1975; Spence, 1980; Korrat, 1986). This method assumes that travel times of rays which travel from the source region toward a particular recording site is adequately described by first-order perturbations between ray paths. This assumption is correct as long as the source region is sufficiently small (much smaller than the shortest source–receiver distance). We used a set of P-wave arrival time differences as recorded at stations $i = 1, N$ from a reference event R, and a nearby event j. The

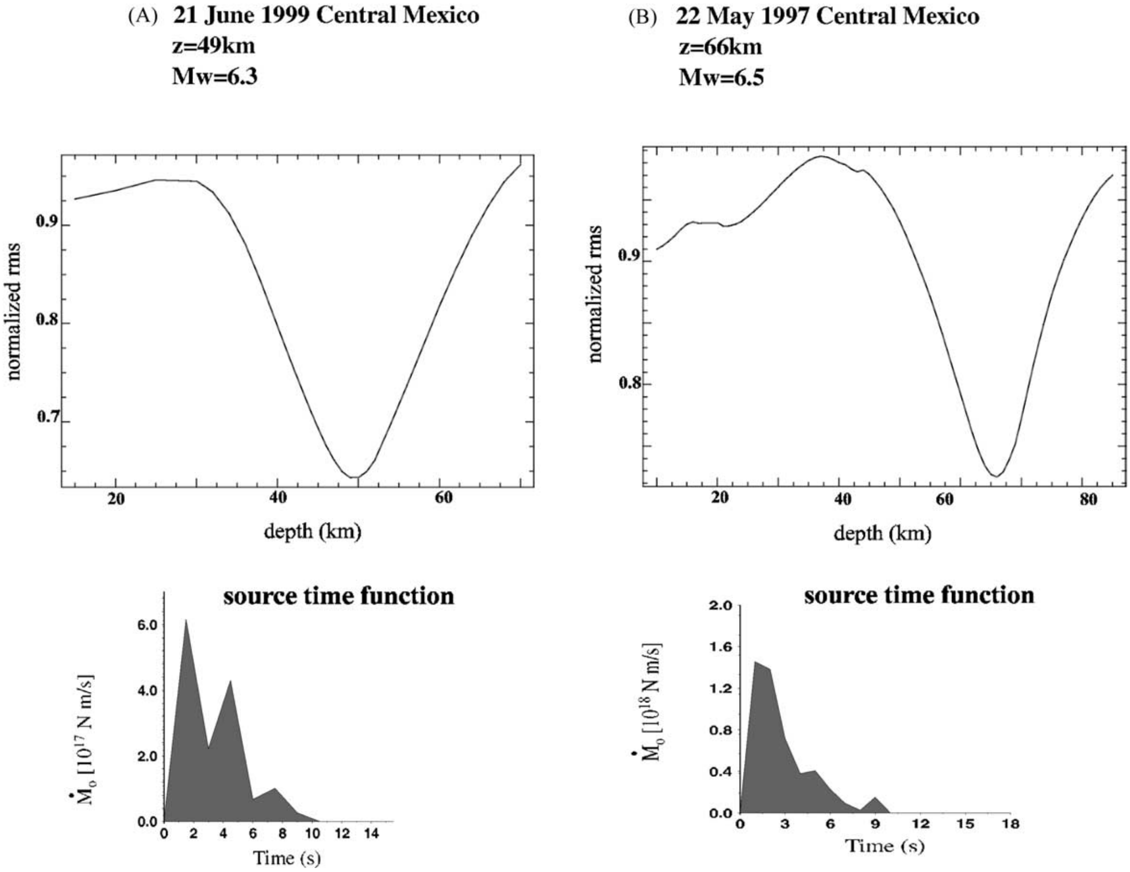

Fig. 2. Two steps of body waveform inversion for two events which occurred in central Mexico. (A) and (B) represent depth and source-time function determination for two Mexican events. Computing inversions for different depths, we calculated the root mean squared residual (rms) between real and synthetic seismograms for each inversion. We choose the depth corresponding to the minimum of the residual. On the lower part of the figure, the source time functions determined for the depth chosen are shown for each event.

differential travel time to the ith station from the master event and jth secondary event (ΔT_{ij}), can be expressed as the difference in origin time (ΔT_{0j}) and first order differences in the ray paths:

$$\Delta T_{ij} = \Delta T_{0j} - \frac{L_j \cos(S_{ij})}{V}$$

where L_j is the distance between the master earthquake and the jth secondary event and S_{ij} the angle formed by a vector joining the two events and a vector tangent to the ray that travels from the focus of the master event to the ith station, V the P-wave speed in the region near the two events. We applied singular value decomposition (SVD) in order to find the solutions of the linearized form of the preceding equation. As slave events are chosen close to the master event, the ray paths to one station from both slave and master events will traverse almost the same structure. As we could not get accurate depth estimates from this method of relocation, we used the depths determined from body wave modelling, so that in fact we did horizontal relative hypocenter location.

We relocated two kinds of earthquakes. In a first step, for larger events ($M_w > 6$), we hand-picked arrivals times of P-waves from digital teleseismic broadband stations of global networks (IRIS and GEOSCOPE). For smaller events ($4.5 < M_w < 6$) we could not get enough broad band readings so that we used the depths and arrival times reported in the earthquake data report (EDR) of the USGS. This method

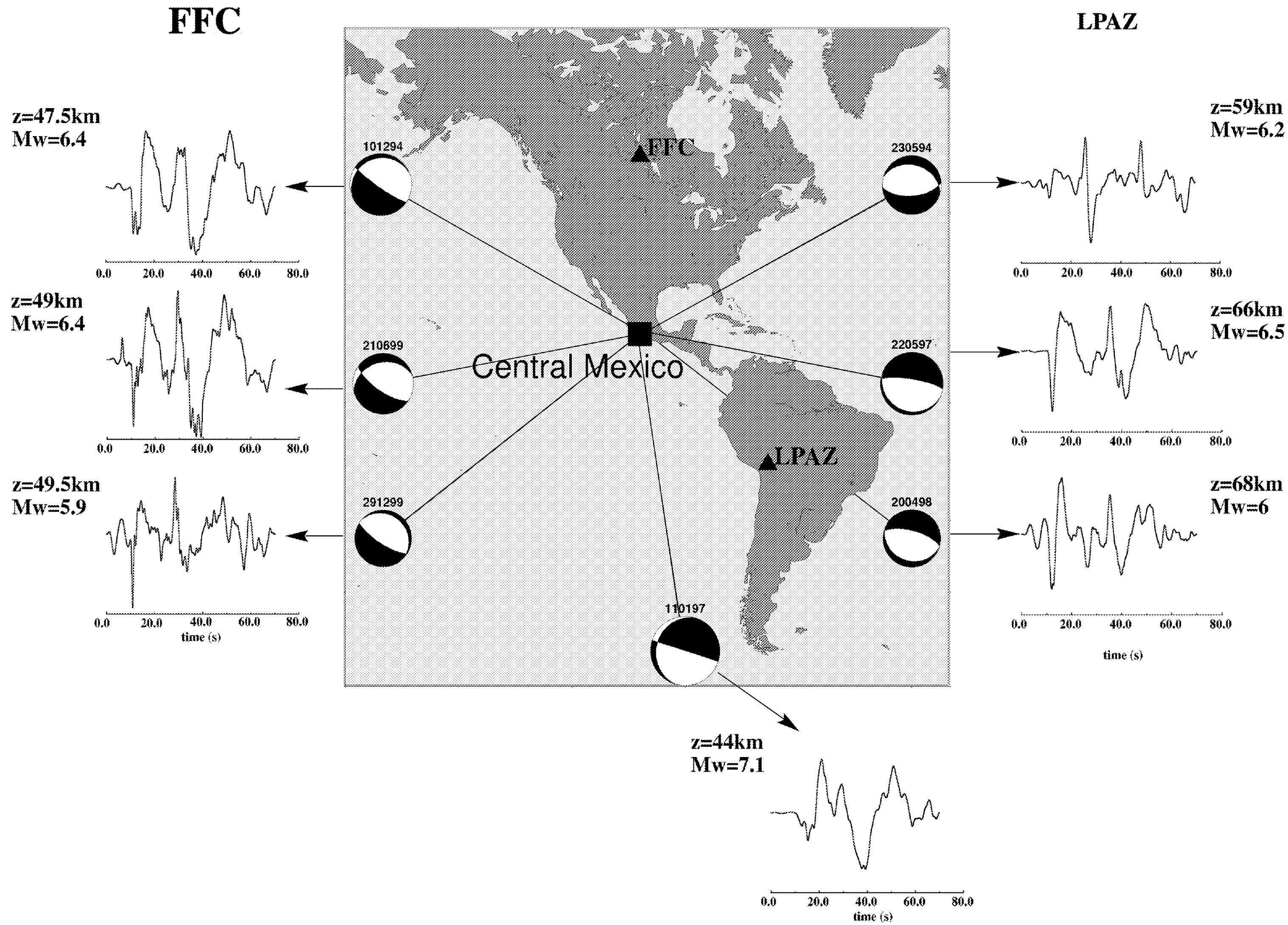

Fig. 3. Displacement seismograms recorded at two stations (FFC and LPAZ) for seven earthquakes in central Mexico. Seismograms for events with the same kind of fault mechanism are shown at the same station (FFC for slab-push events on the left side and LPAZ for slab-pull events on the right side). The dependence on depth and moment is clear if we compare the different phases of signals.

allowed us to obtain an accurate horizontal location of some events in one particular region. As we determined very accurately the depth of each earthquake by inverting body waveforms, we then obtain precise 3D locations.

3. The Punitaqui slab-push earthquake in north central Chile

3.1. Tectonic setting

Beneath central Chile between 27 and 33°S, the oceanic Nazca plate descends under the continental South American plate at very shallow angle. This geometry has been studied by Barazangi and Isacks (1976), Isacks and Barazangi (1977), Araujo and Suárez (1994) using seismicity: this segment of the Nazca plate is relatively flat and roughly follows the contours of the lower boundary of the overriding plate without leaving any asthenospheric material between them. There is no quaternary volcanism above this region and no Altiplano (Jordan et al., 1983). This segment of flat subduction is associated with a deep seismically coupled zone (48–53 km) which is not observed in normal dipping subduction zones (Tichelaar and Ruff, 1991). The initial dip of the seismic zone is $16^\circ \pm 2^\circ$ (Tichelaar and Ruff, 1991) before a progressive downward bending down to 80 km of depth where there is an unbending. After that the slab becomes subhorizontal for a distance of about 250 km (Araujo and Suárez, 1994). Finally, after a new downward bend, the downgoing slab subducts at a steeper angle. In north central Chile, the last large thrust event was the $M_w = 7.9$ Illapel earthquake which occurred on 6 April 1943 (Lomnitz, 1971; Kelleher, 1972; Beck et al., 1998). Its estimated rupture zone extends from 30.2 to 32.2°S.

3.2. An unusual sequence of $M_w > 6$ earthquakes

Seven events of magnitude $M_w > 6$ occurred between July 1997 and January 1998 inside the Illapel gap in north central Chile (Lemoine et al., 2001), (Fig. 4). This high level of seismicity in such a small area during only a few months is very unusual (except for aftershock sequences). For this reason, we thought that these events constitute a closely related swarm of seven $M_w > 6$ earthquakes. These events were spread over an area that overlaps the northern half of the rupture zone of the great $M_w = 7.9$ Illapel earthquake of 1943 (Madariaga, 1998). We can describe the sequence of 1997–1998 north central Chile events as two closely related swarms. The first swarm began with the $M_w = 6.7$ 6 July 1997 interplate shallow thrust event ($z = 17$ km) that occurred in the northern part of the rupture area of the great Illapel thrust event of 1943. This thrust event was followed in July 1997 by three others shallow thrust events. These four interplate events followed a cascade pattern propagating southward, offshore. The July thrust seismicity ended near the future location of the largest event of the sequence: the Punitaqui earthquake of October 1997. After two and a half months of quiescence, the second swarm began with the very unusual $M_w = 7.1$ 15 October 1997 Punitaqui earthquake (Fig. 1). This event took place inside the downgoing Nazca plate at 68 km depth, just below the bottom of the coupling zone defined by Tichelaar and Ruff (1991). It was a slab-push event, i.e. an intermediate depth, intraplate earthquake with a downdip compressional mechanism. We observed clear directivity in the SH waves implying that the actual fault plane was almost vertical with rupture beginning at the top of the slab and propagating downwards. The second swarm started after the 15 October slab-push event with two medium-size thrust events of $M_w = 6.2$ and 6.6 that took place on the plate interface just above the October $M_w = 7.1$ event on 3 November 1997 and 12 January 1998 ($z = 49.5$ and 36 km, respectively).

Down-dip compressional events (slab-push) as large as the Punitaqui earthquake of October 1997 which occur inside the downgoing plate near the plate interface are very unusual for Chile. We found a few rare slab-push events in the Harvard CMT catalogue. They are not common and usually they are either too small to be studied using teleseismic body waveform inversion, or too old to get enough digital data. The only other event we could study occurred in southern Chile on 10 October 1994 at a depth of 169 km. One other important event ($M_w = 7.2$) was reported by Astiz and Kanamori (1986): it took place in southern Chile on 8 May 1971 and its depth was 150 km. But these two events are much deeper than that of Punitaqui one. Actually, they took place near the bottom of the Benioff zone beyond the end of the

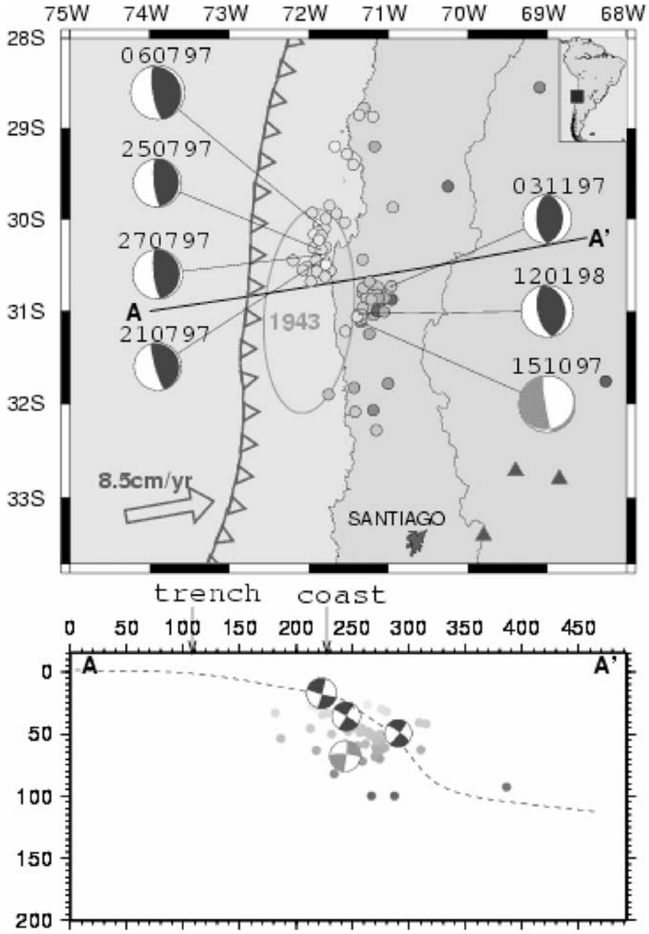

Fig. 4. Inverted $M_w > 6$ focal mechanisms. Focal mechanisms are projected on a vertical cross-section. Dots represent $6 > M_w > 4.5$ relocated earthquakes using a master event method. The darker dots represent deeper earthquakes. Relocations have been made with respect to the largest event of the sequence: the $M_w = 7.1$ Punitaqui earthquake of 15 October 1997 (fault mechanism in the bottom right corner). The sequence can be separated into two swarms. The first swarm of thrust events which followed a cascade pattern towards the south (focal mechanisms on the left). The second swarm began with the occurence of the intraplate compressional slab-push Punitaqui event, followed by two interplate thrust events ($z = 49.5$ and 36 km).

strongly coupled zone between the Nazca and South American plates. They were not considered from the present study.

3.3. Evidence for earthquake interaction

The context of the occurence of the slab-push Punitaqui earthquake is very unusual. The high level of interplate thrust seismicity that preceded this earthquake just a few tens of kilometers from it is a possible explanation for its occurrence. We made some static stress changes computations in this region in order to investigate whether the unusual Punitaqui "slab-push" event had been triggered by some stress transfer between the interplate zone and the downgoing plate.

As we mentioned earlier, the July swarm of thrust events on the subduction interface followed a clear cascade pattern from north to south. These events were almost certainly triggered by each other producing a migration of seismicity from north to south. Since the initial state of stress is unknown, we considered the Coulomb failure stress changes, $\Delta\sigma_f$ which can be expressed as follows:

$$\Delta\sigma_f = \Delta\tau + \mu(\Delta\sigma_n + \Delta P)$$

where $\Delta\tau$ is the shear stress change on a fault. $\Delta\tau$ is positive in the direction of fault slip. $\Delta\sigma_n$ is the normal stress change which is positive if the fault is unclamped. μ is the friction coefficient and ΔP the pore pressure change in the fault zone (it is positive in compression). Usually, the influence of ΔP on $\Delta\sigma_n$ is taken into account using a reduced effective friction coefficient (μ') (Reasenberg and Simpson, 1992; Simpson and Reasenberg, 1994; King et al., 1994; Stein, 1999). An earthquake can change the chance of occurrence of failure on optimally oriented faults in its neighbourhood. Faults are more likely to break if the Coulomb failure stress change $\Delta\sigma_f$ is positive, and failure is discouraged if it is negative. Okada's formulation is used to estimate stress transmitted by an earthquake on the fault (Okada, 1992). The stress transfer is calculated for slip corresponding to

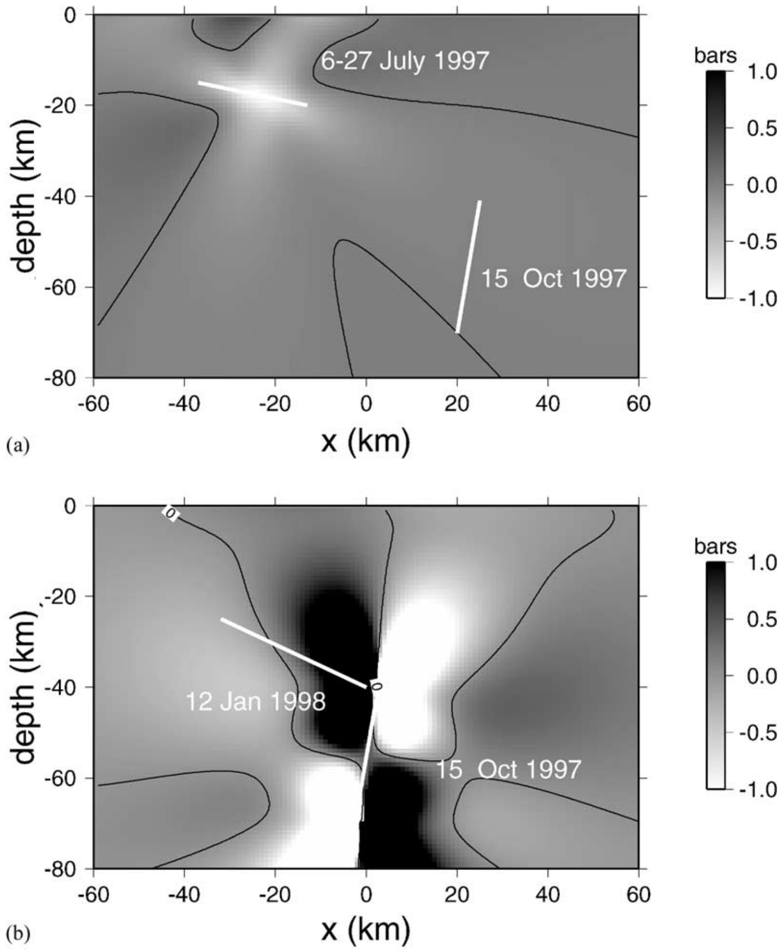

Fig. 5. (a) Coulomb stress changes produced by the July swarm of thrust events along a cross section parallel to the direction of convergence drawn on the location of the Punitaqui slab-push event of 15 October 1997 (see Fig. 4). Coulomb stress change was computed on planes parallel to the vertical nodal plane of the 15 October 1997 earthquake. This event occurred in a region where there is no increase of the Coulomb stress. (b) Same representation as above. Coulomb stress changes produced by the Punitaqui slab-push event on fault planes parallel to that of the 12 January 1998 event. This thrust event is on a region where there is an increase of the Coulomb stress. It was enhanced by the slab-push event.

a dislocation in an elastic medium. We use the dislocation code (DLC) for our computations (Simpson and Reasenberg, 1994).

It was clear from our computations that the change in Coulomb failure stress produced by the ensemble of July events can not explain the occurrence of the 15 October 1997 Punitaqui earthquake (Fig. 5). Coulomb failure stress did not increase on the sub-vertical fault plane of the Punitaqui event. So, we could not explain the occurrence of the Punitaqui event by static stress transfer produced by the unusually high interplate thrust seismicity level of July 1997. On the other hand, the Coulomb failure stress change produced by the slab-push Punitaqui event favored the occurrence of the 3 November 1997 and 12 January 1998 thrust events which took place at the plate interface just above it. Thus, the static stress modelling has demonstrated that there is interaction within each swarm, but it can not explain the occurrence of the intermediate intraplate compressional Punitaqui event after the thrust event swarm of July 1997 (Lemoine et al., 2001).

4. Central Mexico

4.1. Tectonic setting

The subduction of the oceanic Cocos plate beneath the North American lithosphere along the Middle American Trench is complex. Its morphology has been studied by many authors using different methods such as hypocentral distribution of earthquakes either teleseismically recorded (Burbach et al., 1984; Singh and Mortera, 1991; Pardo and Suárez, 1995), or locally recorded (Stolte et al., 1986; Suárez et al., 1990; Singh et al., 1993; Núñez-Cornú and Sánchez-Mora, 1999; Núñez-Cornú et al., 2000), seismic refraction experiments (Valdes et al., 1986; Nava et al., 1988; Cordoba et al., 1993; Núñez-Cornú and Nava, 1993) and gravimetric and magnetotelluric studies (Arzate et al., 1995). Burbach et al. (1984) proposed that the subducted Cocos plate can be divided into segments with common features. Subduction under Mexico is commonly divided in four segments on the basis of the seismicity, focal mechanisms and the geometry of the downgoing slab (Singh and Mortera, 1991; Pardo and Suárez, 1995). From north-west to south-east, this segments are the Jalisco region where the Rivera plate subducts beneath Mexico, and the Michoacan, Guerrero and Oaxaca regions where the Cocos plate subducts beneath Mexico. These segments are bounded approximately by major bathymetric features.

Despite this segmentation, the depth and dip of the shallow interplate interface between the Cocos plate and Mexico change very little along strike. Shallow thrust events all have depth less than 25 km (Pardo and Suárez, 1995). But at depths greater than 30 km, there are lateral variations in the dip angle of the slab. Unfortunately, because of the scarcity of intermediate depth earthquakes west of 99 °W (i.e. West of Oaxaca region) and sparce coverage from local and regional networks along the coast, the morphology of the Wadati-Benioff zone is poorly known (Burbach et al., 1984; Singh and Mortera, 1991). Our region of interest is located in the extreme east of the Michoacan region, very close to its border with the Guerrero region. There is a controverse regarding the morphology of the downgoing slab in this region. Using seismicity studies, Suárez et al. (1990), Singh et al. (1993), Pardo and Suárez (1995) proposed a subhorizontal slab beneath the Guerrero region: the oceanic Cocos plate penetrates beneath central Mexico with a shallow dip angle and it becomes subhorizontal at a depth of about 50 km beyond about 110 km from the trench and up to about 275 km from the trench. Beyond this distance, the geometry of the slab is not constrained because of a lack of seismic activity. Pardo and Suárez (1995) placed this flat subducting slab between 102 and 98°W, i.e. between the projections on the coast of the Orozco and O'Gorman fracture zones. The flat segment of the downgoing Cocos plate is twice as shallow (50 km as opposed to 100 km) and much shorter (around 150 km as opposed to 250 km) than that of the Nazca plate under central Chile. In Mexico, the overriding North American plate is half as thick as that observed in South America (Suárez et al., 1990). Pardo and Suárez (1995) suggested that from the Guerrero flat segment, the dip angle of the downgoing slab increases eastward and westward at depths greater than 30 km. On the other hand, other authors did not find evidence for a subhorizontal plate under the Guerrero region. Close to our region of interest, Stolte et al. (1986) used the hypocentral distribution of locally recorded aftershocks of the $M_s = 8.1$ Michoacan earthquake of 1985 in order to define the Benioff zone structure as far as approximately 120 km from the trench. They defined the subduction interface as a nearly planar structure dipping at approximately 14°. But they noticed a sudden increase in the depth of hypocenters around 110 km inland. Váldes-Gonzalez and Meyer (1996) obtained a dip angle of 10° until 150 km from the trench. Cordoba et al. (1993), González et al. (1997) found also shallow-dipping subduction without unbending down to 150 km from refraction profiles.

Earthquakes we studied occurred west of the supposed flat subduction where the geometry of the subduction is still poorly constrained. They were preceded by large thrust events in 1979 ($M_w = 7.6$), 1981 ($M_w = 7.4$) and 1985 ($M_w = 8.0$ and 7.6).

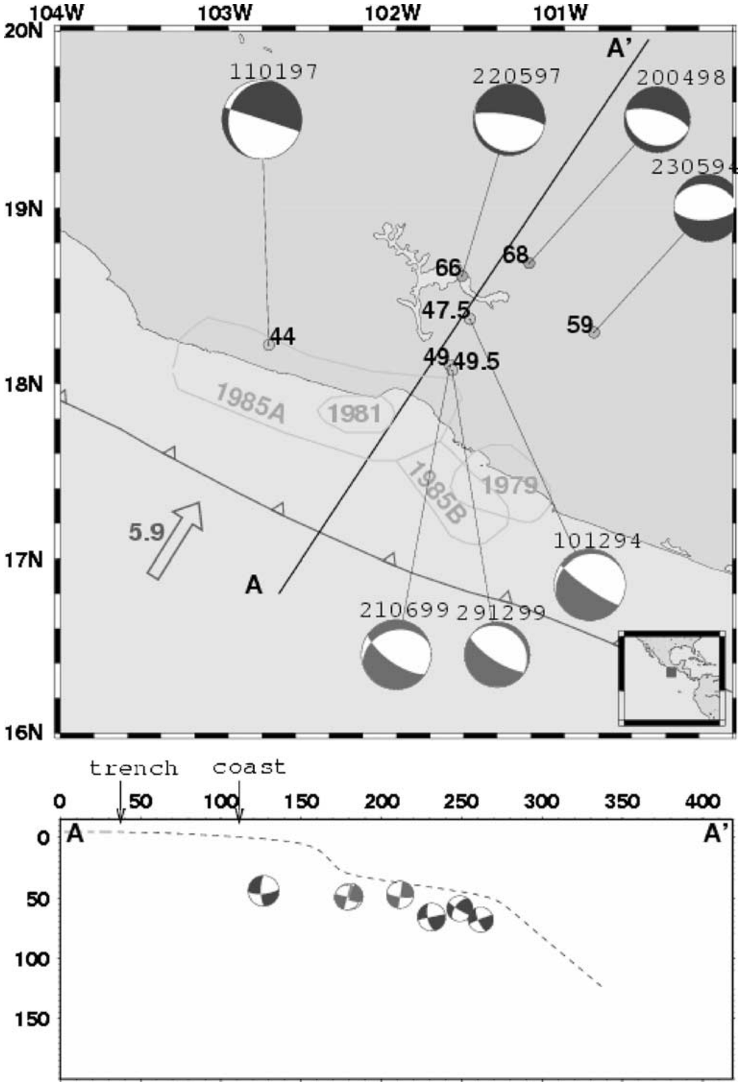

Fig. 6. Intermediate depth seismicity in central Mexico. Events were relocated using a master event method. Fault mechanisms were determined using body waveform inversions. Depth is given by the dark numbers. The rupture zones of the last large thrust earthquakes in central Mexico are indicated (from Mikumo et al., 1999). The dotted line on the cross-section correspond to the supposed geometry of the Cocos plate from Pardo and Suárez (1995). Earthquakes can be separated into two groups: three events drawn on the lower part of the figure are intraplate compressional events whereas the four others are extensional events. Except the 11 January 1997 event, slab-pull events occurred deeper than the slab-push ones.

4.2. Unusual intermediate depth seismicity between 1994 and 1999

Beneath central Mexico, there was a high level of intermediate depth seismicity between 1994 and 1999 in a confined area. Seven intraplate intermediate depth earthquakes with magnitude between $M_w = 5.9$ and 7.1 occurred inland in the subducted Cocos plate. This intraplate intermediate depth seismicity is particularly unusual in this region northwest of 99 °W where there is a lack of intermediate depth earthquakes. We applied body waveform inversions in order to obtain the source parameters and relative relocations for this group of events. We can separate these seven earthquakes into two groups (Fig. 6).

The first group was composed of three earthquakes that occurred downdip of the interplate coupled zone at depths between 47.5 and 49.5 km. These three events have a P-axis which follows the dip-direction of the downgoing subducted plate, i.e. they are slab-push events. These compressional earthquakes occurred on 10 December 1994 (Zihuatanejo $M_w = 6.6$ earthquake see Cocco et al. (1997) and Quintanar et al. (1999)), and on 21 June and 29 December 1999 $M_w =$ 6.4 and 5.9, respectively (Singh et al., 2000). For the Zihuatanejo earthquake, the prefered fault plane was determined by Cocco et al. (1997): it was the subvertical one (azimuth of 130°, dip of 79° and rake of −86°).

The four other earthquakes had tensional mechanisms. The largest event occurred very close to the coast on 11 January 1997 ($M_w = 7.1$). It was accurately studied by Mikumo et al. (1999, 2000). It occurred next to the northern border of the rupture area of the large Michoacan 1985 earthquake. The three other intraplate extensional events took place farther inland and deeper. They occurred on 23 May 1994 ($M_w =$ 6.2, $z = 59$ km), 22 May 1997 ($M_w = 6.5$, $z =$ 66 km) and 20 April 1998 ($M_w = 6.0$, $z = 68$ km).

5. Preliminary results from central Peru

5.1. Tectonic setting

Peru is located on the well-defined seismic belt of the Peru-Chile arc. It is characterized by high seismic activity and a deep trench. The relatively young (around 50 Million years old) Nazca plate subducts under the overriding South American plate with an approximate convergence velocity of 7.8 cm per year in direction 80°N (DeMets et al., 1990). The subducted Nazca plate shows a lateral variation in dip. From latitude 15°S down to 27°S in northern Chile, the Benioff zone has a dip of 30°. But beneath northern and central Peru, subduction takes place with a low dip angle. Several studies of the seismicity of this subduction zone have been made in order to constrain the geometry of the downgoing slab (Stauder, 1975; Barazangi and Isacks, 1976, 1979; Isacks and Barazangi, 1977; Suárez et al., 1990; Gutscher et al., 2000). The Nazca plate subducts under northern and central Peru at a shallow angle which steepens progressively. At a depth of about 100 km, very close to the Pacific coast, the slab unbends and becomes sub-horizontal for a distance of approximately 300 km. Then, the Nazca plate bends a last time to finally dip very steeply. The southern and northern limits of the flat segment seem to be controlled by the existence of aseismic structural features (the Nazca ridge and the Carnegie ridge). These features are probably zones of weakness along which the Nazca plate is being torn. The flat geometry of the slab beneath northern and central Peru is characterized by a lack of Quaternary volcanism. When it descends, the slab follows the contours of the overriding South American plate without allowing the presence of asthenospheric material between the two plates.

We studied more particularly earthquakes in central Peru. This region is characterized by a complex pattern of seismicity. To the North, all the rupture zones end at about 10°S, where the Mendaña fracture zone enters into the subduction zone, for example, the large interplate thrust events in 1746 ($M = 8.4$), 1940 ($M_w = 8.1$), 1966 ($M_w = 7.7$) (Dorbath et al., 1990). There are also many intraplate, intermediate depth earthquakes such as the very destructive 31 May 1970 $M_w = 8.0$ earthquake (Abe, 1972; Stauder, 1975; Dewey and Spence, 1979; Beck and Ruff, 1989).

5.2. Very important intermediate depth seismicity in central Peru

The CMT catalogue from Harvard shows a very high level of intermediate depth seismicity in Peru,

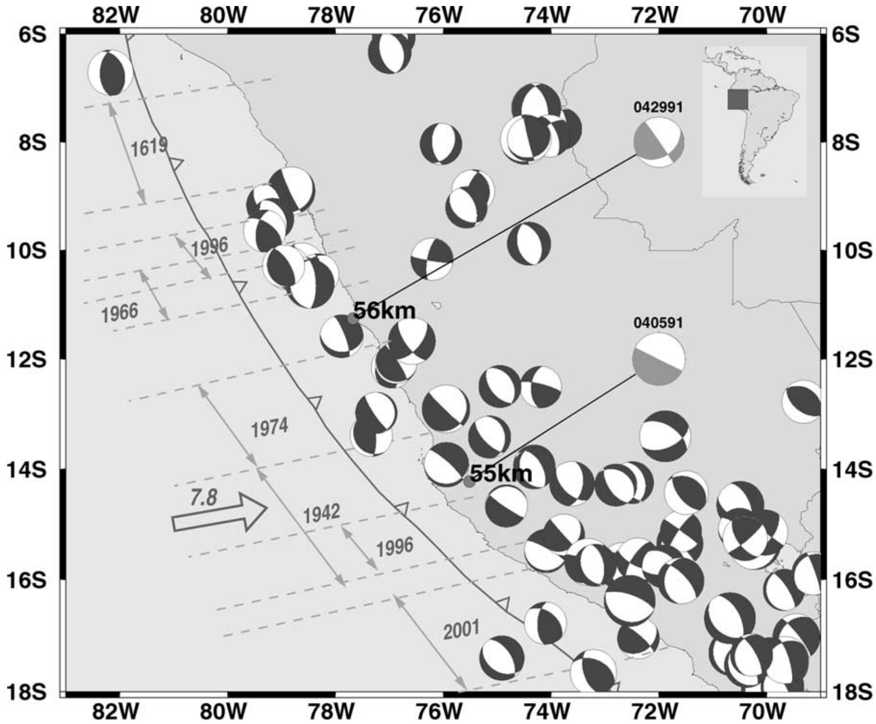

Fig. 7. $M_w > 5.5$ moment tensors solutions from 1977 to 2000 obtained from the Harvard CMT catalog at intermediate depth (40 km < z < 300 km). Thin arrows represent approximate rupture areas of the last large thrust events. Two slab-push events have been modeled (29 April 1991 and 5 April 1991). Depth is indicated by the dark numbers. This very high level of intermediate depth seismicity contains both compressional and extensional intraplate earthquakes.

with both compressional and extensional events. Unfortunately, only two events could be studied using teleseismic digital stations (Fig. 7). We applied teleseismic body waveform inversion in order to obtain the source parameters of these earthquakes which occurred on 5 and 29 April 1991 ($M_w = 6.3$ and 5.9, respectively). We found that these two events occurred inside the downgoing plate. Their depths were 55 and 56 km, respectively and they had down-dip compressional mechanisms (slab-push). They occurred very close to the coast.

North of these two events, next to the location of the large 1966 thrust event, occurred the large 31 May 1970 intraplate normal faulting event ($M_s = 7.8$, $z = 64$ km (Dewey and Spence, 1979)). The relocated aftershocks of the 1970 event form two clusters (Dewey and Spence, 1979). The first cluster lies on the location of the main shock of 31 May. In this cluster, the aftershocks have similar focal mechanism to the main shock and are characterized by down-dip tension. The second cluster was larger and focal mechanisms of the aftershocks were down-dip compressional (Fig. 8), and three largest aftershocks belonged to this second cluster ($z = 54$, 55 and 47 km). This cluster was located approximately 50–60 km southeast from the main shock epicenter (Stauder, 1975; Dewey and Spence, 1979). Beck and Ruff (1989) divided the main shock into two subevents: during the first 40 s, the first subevent occurred at 50 km depth with a down-dip tensional mechanism, then the second subevent occurred at 30 km depth with a down-dip compressional mechanism (depths shallower than the one determined by Dewey and Spence (1979), i.e. 64 km). Aftershock complexity reflected the main shock complexity. We noted that the down-dip compressional aftershocks of the second cluster represent the same kind of events as those we studied using body waveform inversion (5 and 29 April 1991).

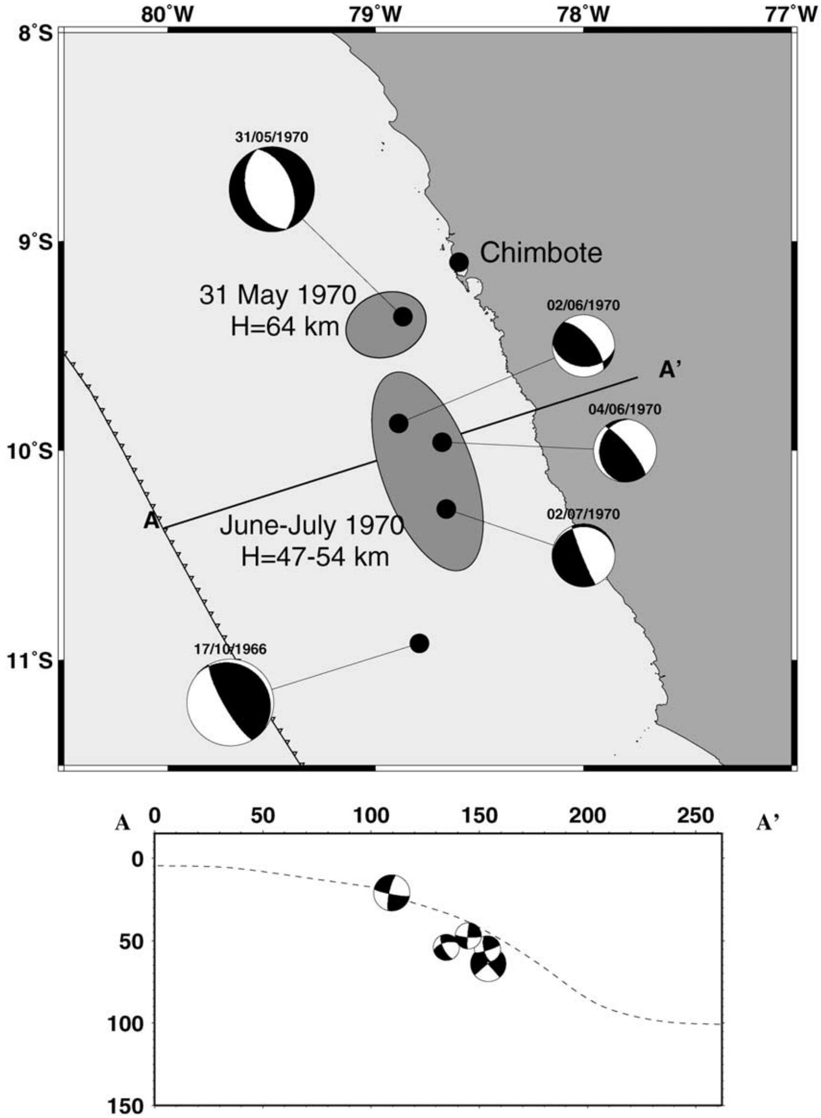

Fig. 8. Focal mechanisms from Stauder (1975) and aftershock clusters from Dewey and Spence (1979) for the $M_w = 7.9$ earthquake of 31 May 1970. This was an intraplate extensional event whereas the June–July cluster was composed of several intraplate compressional events. These intraplate earthquakes occured next to the rupture area of the $M_w = 8.1$, 17 October 1966 underthrusting event. The dotted line represents the approximate shape of the oceanic Nazca plate from Gutscher et al. (2000).

6. Discussion

The purpose of this study was to try to understand what phenomena can explain the occurrence of intraplate intermediate depth earthquakes in three distinct subduction zones: north central Chile, central Mexico and central Peru. Are they due to stress transfer during the earthquake cycle as suggested by Astiz and Kanamori (1986), Astiz (1987), Astiz et al. (1988), Lay et al. (1989), Dmowska et al. (1988, 1996), or to stress transfer due to the bending inside these slabs?

We studied one $M_w = 7.1$ slab-push event in north central Chile—the Punitaqui earthquake of 15 October 1997—which took place at the top of the downgoing subducted plate where the unbending of the Nazca plate should produce compressional stresses. Coulomb stress changes calculations showed that the swarm of interplate thrust events occurring three months before the Punitaqui slab push event just a few tens of kilometers from it was not large enough to trigger this down-dip compressional event. Moreover, the duration of the earthquake cycle in this region is around 100 years. Around Illapel region, the last large thrust event occurred in 1943. The subduction is then approximately at the middle of the earthquake cycle. At intermediate depth, the downgoing slab should undergo compressional stresses at the beginning of the earthquake cycle and tensional stresses at the end (Astiz and Kanamori, 1986). But can the earthquake cycle determine the state of stress in the Illapel region?

We also studied two slab-push earthquakes which occurred beneath central Peru. These events occurred respectively down-dip of the large thrust events of 1974 and 1942. They both had approximately the same location inside the downgoing Nazca plate than the slab-push Punitaqui event of north central Chile: they were located at the top of the plate where it bends upward before it flattens (Fig. 9). Several authors have studied the very interesting sequence of intraplate intermediate depth events which occurred in 1970 after the 1966 large thrust event. In 31 May 1970, an intermediate depth earthquake occurred inside the oceanic Nazca plate. It had a complex dual focal mechanism (Beck and Ruff, 1989). The first subevent had a downdip extensional focal mechanism at depth 50 km whereas the second subevent occurred at $z = 30$ km with a downdip compressional focal mechanism. Moreover, aftershocks of the 31 May 1970 earthquake can be separated in two different clusters: the first one was close to the main shock and the second one was larger and caracterised by compressional intraplate events.

Next to Guerrero, we studied several intermediate depth earthquakes. Four were slab-pull events and three were slab-push ones. The shallower event (11 January 1997) was studied by Mikumo et al. (1999) who computed coseismic stress changes induced by the 1985 Michoacan earthquake ($M_w = 8.1$). He showed that the large extensional event of 11 January 1997 took place in the zone of maximum coseismic stress increase. It is not possible to explain in the same way the other intermediate depth earthquakes as they occurred inland, farther from the interplate coupled zone. The three slab-push events were shallower ($z = 47.5$, 49 and 49.5 km) and closer to the coast than the three slab-pull events ($z = 59$, 66 and 68 km). In this region, the last large thrust event was the 1985 Michoacan earthquake. Thus, this subduction area is also at the beginning of the earthquake cycle, so that at intermediate depth the Cocos plate should be under compression, but there were as many down-dip extensional events as down-dip compressional ones. Under central Mexico, the geometry of the subducted Cocos plate is poorly constrained. But the hypothesis of a flat slab under this region proposed by Suárez et al. (1990), Singh et al. (1993) and Pardo and Suárez (1995) could explain that both compressional and extensional events occur almost simultaneously. Moreover, Gardi et al. (2000) was forced to introduce this flexured geometry in order to explain the occurence of the 10 December 1994 Zihuatanejo earthquake using dynamic modelling of the subduction zone. According to the hypothesis of a flat slab beneath central Mexico, the flat segment of the downgoing oceanic plate is shorter than beneath north central Chile and north and central Peru (around 150 km beneath central Mexico and around 300 km beneath central Peru and 250 km beneath north central Chile). The flat segment is preceded by a concave curvature (compression at the top of the slab and extension at the bottom) and followed by a convex curvature (extension at the top of the slab and compression at the bottom). If the flat segment dips slightly, the geometry of the subducted plate could explain the intermediate depth seismicity we observed between 1994 and 1999. The three shallower down-dip compressional earthquakes were located close to the top of the concave bend and the three down-dip extensional events were located close to the top of the convex bend ending the flat segment (Fig. 9). Singh et al. (2000) studied intraplate earthquakes under central Mexico since 1964. They also suggested that the slab-push events of 12 December 1994, 21 June 1999 and 29 December 1999 can be related to the bending and unbending of the slab in this region.

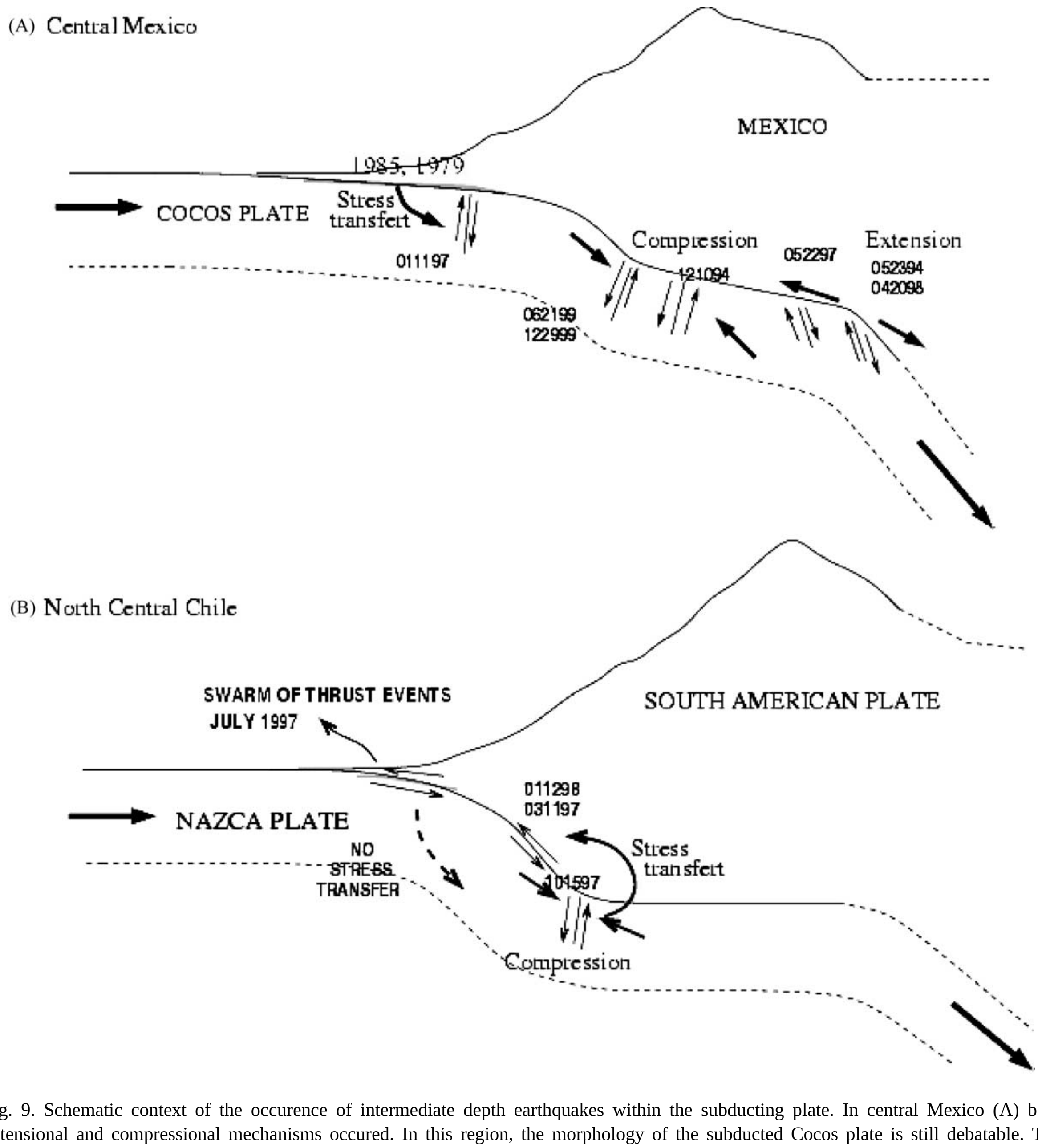

Fig. 9. Schematic context of the occurence of intermediate depth earthquakes within the subducting plate. In central Mexico (A) both extensional and compressional mechanisms occured. In this region, the morphology of the subducted Cocos plate is still debatable. The dotted line corresponds to the shape of the slab proposed by Pardo and Suárez (1995). Mikumo et al. (1999) explained the occurence of the 11 January 1997 extensional event by the coseismic stress increase generated by the 1985 thrust event. Intraplate intermediate depth compressional and extensional events could be associated with unbending and bending of the Cocos plate. In north central Chile (B), Coulomb stress changes calculations could not explain the occurence of the Punitaqui slab-push event (15 October 1997). The Punitaqui slab-push event was located at the top of the Nazca plate, where bending is upward (i. e. the same situation as in Peru).

7. Conclusion

For the three subduction zones of north central Chile, central Mexico and central Peru, the temporal link between large intraplate intermediate depth earthquakes we studied does not seem to provide an explanation for the intermediate depth earthquakes we studied. Taylor et al. (1996) observed that while there is a clear time-in-cycle dependence of outer rise seismicity, the subducted slab at intermediate depth may have a much more complex stress field. At this depth, the slab may undergo thermal stressing, dehydration, asthenospheric relative motion, unbending and, possibly loading from the weight of the thick overriding continental plate that may produce local deviatoric stresses. These phenomena could explain the occurrence of both compressional and extensional stresses. At intermediate depth, the tendency of extensional seismicity to occur prior to a large interplate thrust event, and of compressional seismicity to occur after such events which has been observed by large scale studies of the seismicity pattern in subduction zones (Lay et al., 1989) may be complicated by other effects, especially in flat subduction zones. In these flat subduction zones, the subducted oceanic plate undergoes three flexures before sinking in the asthenosphere at depth greater than 100 km. Isacks and Barazangi (1977) gave an example of elastic stress difference induced by a radius of curvature of 200 km of a 20 km thick plate, which would be as large as 50 kilobars. Using dynamic modelling of the flat subduction zone in central Mexico, Gardi et al. (2000) suggested that the stress pattern is very sensitive to the geometry of the plates. They found that for this geometry of the subducted slab, and for a partial stress drop, the main thrust earthquakes do not invert the polarity of the stress field which is compressional above the down-dip edge of the main thrust zone and extensional below. Moreover, intraplate intermediate depth seismicity could be influenced by the tensional stress induced by the heavy sinking oceanic slab. But since beneath north central Chile, central Peru and central Mexico, the Nazca and Cocos plates are relatively young (so have a small negative buoyancy), while the convergence rate is large—7.8 cm per year in Peru, 8.4 cm per year in central Chile and 6 cm per year in Mexico (DeMets et al., 1990)—so that the tendency to sink is expected to be small (Fujita and Kanamori, 1981). Thus the slab-pull due to the sinking of the downgoing slab may be reduced in these regions, so that other effects of subduction may be predominant, such as bending and unbending of the slab in north central Chile, central Peru and central Mexico (if we use the debated hypothesis of a flat slab under central Mexico). The predominance of the effect of the geometry of the slab could allow the occurrence of both compressional and extensional earthquakes in these subduction zones. The slab-push and slab-pull events we studied seem to be related to the heterogeneity of the stress field inside flexed downgoing slabs.

Acknowledgements

We would like to thank Massimo Cocco, Ross Stein, Renata Dmowska, James Rice, for usefull discussions. We also thank the reviewers Francisco Javier Núñez-Cornú and Jaime Yamamoto for constructive and critical comments which helped us to improve the manuscript. This research was partially supported by ECOS/CONICYT contract C97U01 and FONDECYT contract 1990036.

References

Abe, K., 1972. Mechanisms and tectonic implications of the 1966 and 1970 Peru earthquakes. Phys. Earth Planet. Inter. 5, 367–379.

Araujo, M., Suárez, G., 1994. Geometry and state of stress of the subducted Nazca plate beneath central Chile and Argentina: evidence from teleseismic data. Geophys. J. Int. 116, 283–303.

Arzate, J.A., Mareschal, M., Livelybrooks, D., 1995. Electrical image of the subducting Cocos plate from magnetotelluric observations. Geology 23, 703–706.

Astiz, L., Kanamori, H., 1986. Interplate coupling and temporal variation of mechanisms of intermediate-depth earthquakes in Chile. Bull. Seismol. Soc. Am. 76, 1614–1622.

Astiz, L., 1987. Source analysis of large earthquakes in Mexico and study of intermediate-depth earthquakes and interplate seismic coupling. Ph.D. Thesis. California Institute of Technology, Pasadena, USA.

Astiz, L., Lay, T., Kanamori, H., 1988. Large intermediate depth earthquakes and the subduction process. Phys. Earth Planet. Inter. 53, 80–166.

Barazangi, M., Isacks, B.L., 1976. Spatial distribution of earthquakes and subduction of the Nazca plate beneath South America. Geology 4, 686–692.

Barazangi, M., Isacks, B.L., 1979. Subduction of the Nazca plate beneath Peru: evidence from spatial distribution of earthquakes. Geophys. J. R. Astro. Soc. 57, 537–555.

Beck, S.L., Ruff, L.J., 1989. Great earthquakes and subduction along the Peru trench. Phys. Earth Planet. Inter. 57, 199–224.

Beck, S., Barrientos, S., Kausel, E., Reyes, M., 1998. Source characteristics of historic earthquakes along the central Chile subduction zone. J. South Am. Earth Sci. 11, 115–129.

Burbach, G.V., Frohlich, C., Pennington, W.D., Matumoto, T., 1984. Seismicity and tectonics of the subducted Cocos plate. J. Geophys. Res. 89, 7719–7735.

Christensen, D.H., Ruff, L.J., 1983. Outer-rise earthquakes and seismic coupling. Geophys. Res. Lett. 10, 697–700.

Christensen, D.H., Ruff, L.J., 1985. Analysis of the trade-off between hypocentral depth and source time function. Bull. Seism. Soc. Am. 75, 1637–1656.

Christensen, D.H., Ruff, L.J., 1988. Seismic coupling and outer rise earthquakes. J. Geophys. Res. 93, 13421–13444.

Cocco, M., Pacheco, J., Singh, S.K., Courbouleix, F., 1997. The Zihuatanejo, Mexico, earthquake of 10 December 1994 ($M = 6.6$): source characteristics and tectonic implications. Geophys. J. Int. 131, 135–145.

Cordoba, D., Gonzalez, A., Núñez-Cornú, F.L., Nava, F., Gonzalez, L., Blanco, M.J., Pous, J., Graniel, J., Yamamoto, J., Mota, R., Castellanos, G., Sanchez, C., Calderon, G., 1993. Structure of the crust along the coast of Guerrero, Mexico. Seismol. Res. Lett. 64, 40.

Demets, C., Gordon, R.G., Argus, D.F., Stein, S., 1990. Current plate motions. Geophys. J. Int. 101, 425–478.

Dewey, J.W., Spence, W., 1979. Seismic gaps and source zones of recent large earthquakes in coastal Peru. Pageoph. 117, 1148–1171.

Dmowska, R., Rice, J.R., Lovison, L.C., Josell, D., 1988. Stress transfer and seismic phenomena in coupled subduction zones during the earthquake cycle. J. Geophys. Res. 93, 7869–7884.

Dmowska, R., Zheng, G., Rice, J.R., 1996. Seismicity and deformation at convergent margins due to heterogeneous coupling. J. Geophys. Res. 101, 3015–3029.

Dorbath, L., Cisternas, A., Dorbath, C., 1990. Assesment of the size of large and great historical earthquakes in Peru. Bull. Seismol. Soc. Am. 80, 551–576.

Dziewonski, A.M., Ekström, G., Maternovskaya, N.N., 2001. Centroïd-moment tensor solutions for July–September 2000. Phys. Earth Planet. Inter. 124, 9–23.

Fitch, T.J., 1975. Compressional velocity in source regions of deep earthqukes: an application of the master earthquake technique. Earth Planet. Sci. Lett. 26, 156–166.

Fujita, K., Kanamori, H., 1981. Double seismic zones and stresses of intermediate depth earthquakes. Geophys. J. R. Astro. Soc. 66, 131–156.

Gardi, A., Cocco, M., Negredo, A.M., Sabadini, R., Singh, S.K., 2000. Dynamic modelling of the subduction zone of central Mexico. Geophys. J. Int. 143, 809–820.

González A., Núñez-Cornú F., Córdoba, D., 1997. Estructura sísmica de la corteza entre la Costa de Guerrero y el Centro de México. GEOS 17, 284.

Gutscher, M.A., Spakman, W., Bijwaard, H., Engdahl, E.R., 2000. Geodynamics of flat subduction: seismicity and tomographic constraints from the Andean margin. Tectonics 19, 814–833.

Hernandez, B., Shapiro, N.M., Singh, S.K., Pacheco, J.F., Cotton, F., Campillo, M., Iglesias, A., Cruz, V., Gómez, J.M., Alcántara, L., 2001. Rupture history of 30 September 1999 intraplate earthquake of Oaxaca, Mexico ($M_w = 7.5$) from inversion of strong-motion data. Geophys. Res. Lett. 28, 363–366.

Isacks B.L., Barazangi, M., 1977. Geometry of Benioff zones: lateral segmentation and downwards bending of the subducted lithosphere. In: Talwani, M., Pitman, W. (Eds.), Islands Arcs, Deep Sea Trenches and Back Arc Basins. American Geophysical Union, Ewing Series 1, pp. 99–114.

Jordan, T.E., Isacks, B.L., Allmendinger, R.W., Brewer, J.A., Ramos, V.A., Ando, C.J., 1983. Andean tectonics related to geometry of subducted Nazca plate. Geol. Soc. Am. Bull. 94, 341–361.

Kelleher, J.A., 1972. Rupture zones of large South American earthquakes and some predictions. J. Geophys. Res. 77, 2087–2103.

King, G.C.P., Stein, R.S., Lin, J., 1994. Static stress changes and the triggering of earthquakes. Bull. Seism. Soc. Am. 84, 935–953.

Korrat, I., 1986. Mécanisme et distribution spatiale des épicentres en relation avec la rupture de la lacune de Valparaiso (Chili) en mars 1985. Ph.D. Thesis. Université Paris 7, France.

Lay, T., Astiz, L., Kanamori, H., Christensen, D.H., 1989. Temporal variation of large intraplate earthquqkes in coupled subduction zones. Phys. Earth Planet. Inter. 54, 258–312.

Lemoine, A., Madariaga, R., Campos, J., 2001. Evidence for earthquake interaction in central Chile: the July 1997–September 1998 sequence. Geophys. Res. Lett. 28, 2743–2746.

Lomnitz, C., 1971. Grandes terremotos y tsunamis en Chile durante el periodo 1535–1955. Geofis. Panam. 1, 151–178.

Madariaga, R., 1998. Sismicidad de Chile. Física de la Tierra 10, 221–258.

Malgrange, M., Deschamps, A., Madariaga, R., 1981. Trust and extensional faulting under the Chilean coast: 1965, 1971 Aconcagua earthquakes. Geophys. J. R. Astro. Soc. 66, 313–332.

Malgrange, M., Madariaga, R., 1983. Complex distribution of large thrust and normal fault earthqukes in the Chilean subduction zone. Geophys. J. R. Astro. Soc. 73, 489–505.

Mikumo, T., Singh, S.K., Santoyo, M.A., 1999. A possible stress interaction between large thrust and normal faulting earthquakes in the Mexican subduction zone. Bull. Seismol. Soc. Am. 89, 1418–1427.

Mikumo, T., Santoyo, M.A., Singh, S.K., 2000. Dynamic rupture and stress change in a normal faulting earthquake in the subducting Cocos plate. Geophys. J. Int. 140, 611–620.

Nábělek J., 1984. Determination of earthquake source parameters from inversion of body waves. Ph.D. Thesis. MIT, USA.

Nábělek J., 1985. Geometry and mechanism of faulting of the 1980 El Asnam, Algeria, earthquake from inversion of teleseismic body waves and comparison with field observations. J. Geophys. Res. 90, 12713-12728.

Nava F., Núñez-Cornú, Córdoba, F.L.D., Mena, M., Ansorge, J., González, J., Rodríguez, M., Banda, E., Mueller, S., Udías, A., García-García, M., Calderón, G. 1988. Structure of the

Middle America Trench in Oaxaca, Mexico. Tectonophysics 154, 241-251.
Núñez-Cornú F.J., Nava, F., 1993. P-wave velocity structure of the coast of Oaxaca, Mexico. Seismol. Res. Let. 64, 40.
Núñez-Cornú F.J., Sánchez-Mora, C., 1999. Stress field estimations for Colima Volcano, Mexico, based on seismic data. Bull. Volcanol. 60, 568-580.
Núñez-Cornú F.J., Rutz, M., Reyes-Dávila, G., Nava, F.A., Suarez-Plascencia, C., 2000. Characteristics of seismicity in the coast and north of Jalisco block, Mexico. EOS Transc. 81, F910.
Okada, Y., 1992. Internal deformation due to shear and tensile faults in a half-space. Bull. Seism. Soc. Am. 82, 1018–1040.
Pardo, M., Suárez, G., 1995. Shape of the subducted Rivera ans Cocos plates in southern Mexico: seismic and tectonic implications. J. Geophys. Res. 100, 12357–12373.
Quintanar, L., Yamamoto, J., Jiménez, Z., 1999. Source mechanism of two 1994 intermediate-depth-focus earthquakes in Guerrero, Mexico. Bull. Seism. Soc. Am. 89, 1004–1018.
Reasenberg, P.A., Simpson, R.W., 1992. Response of regional seismicity to the static stress change produced by the Loma Prieta earthquake. Science 255, 1690–1987.
Simpson R.W., Reasenberg, P.A., 1994. Earthquake-induced static stress changes on central California faults. In: Simpson, R.W. (Ed.), The Loma Prieta, California, Earthquake of 17 October 1989—Tectonic Processes and Models. US Geol. Surv. Profess. Pap. 1550-F.
Singh, S.K., Suárez, G., Domínguez, T., 1985. The Oaxaca, Mexico, earthquake of 1931: lithospheric normal faulting in the subducted Cocos plate. Nature 317, 56–58.
Singh, S.K., Mortera, F., 1991. Source time functions of large Mexican subduction earthquakes, morphology of the Benioff zone, age of the plate, and their tectonic implications. J. Geophys. Res. 96, 21487–21502.
Singh, S.K., Pardo, M., 1993. Geometry of the Benioff zone and state of stress in th overriding plate in central Mexico. Geophys. Res. Lett. 20, 1483–1486.
Singh, S.K., Ordaz, M., Pacheco, J.F., Quaas, R., Alcántara, L., Alcocer, S., Gutierrez, C., Meli, R., Ovando, E., 1999. A preliminary report on the Tehuacán, México earthquake of 15 June 1999 ($M_w = 7.0$). Seism. Res. Lett. 70, 489–504.
Singh, S.K., Ordaz, M., Alcántara, L., Shapiro, N., Kostoglodov, V., Pacheco, J.F., Alcocer, S., Gutiérrez, C., Quaas, R., Mikumo, T., Ovando, E., 2000. The Oaxaca earthquake of 30 September 1999 ($M_w = 7.5$): a normal-faulting event in the subducted Cocos plate. Seism. Res. Lett. 71, 67–78.
Singh, S.K., Pacheco, J., Mikumo, T., Kostoglodov, V., 2000. Intraplate earthquakes and their relationship with large great interplate thrust earthquakes. Seism. Res. Lett. 71, 239.
Spence, W., 1980. Relative epicenter determination using P-wave arrival-time differences. Bull. Seism. Soc. Am. 70, 171–183.
Stauder, W., 1973. Mechanism and spatial distribution of Chilean earthquakes with relation to subduction of the oceanic plate. J. Geophys. Res. 78, 5033–5061.
Stauder, W., 1975. Subduction of the Nazca plate under Peru as evidenced by focal mechanisms and by seismicity. J. Geophys. Res. 80, 1053–1064.
Stein, R.S., 1999. The role of stress transfer in earthquake occurrence. Nature 402, 605–609.
Stolte, C., McNally, K.C., González-Ruiz, J., Simila, G.W., Reyes, A., Rebollar, C., Munguía, L., Mendoza, L., 1986. Fine structure of a postfailure Wadati–Benioff zone. Geophys. Res. Lett. 13, 577–580.
Suárez G., Monfret, T., Wittlinger, G., David, C., 1990. Geometry of subduction and depth of the seismogenic zone in the Guerrero gap, Mexico. Nature 345, 336-338.
Suárez, G., Gagnepain, J., Cisternas, A., Hatzfeld, D., Molnar, P., Ocola, L., Roecker, S.W., Viodé, J.P., 1990. Tectonic deformation of the Andes and the configuration of the subducted slab in Peru: results from a microseismic experiment. Geophys. J. Int. 103, 1–12.
Taylor, M.A.J., Zheng, G., Rice, J.R., Stuart, W.D., Dmowska, R., 1996. Cyclic stressing and seismicity at strongly coupled subduction zones. J. Geophys. Res. 101, 8363–8381.
Taylor, M.A.J., Dmowska, R., Rice, J.R., 1998. Upper plate stressing and seismicity in the subduction earthquake cycle. J. Geophys. Res. 103, 24523–24542.
Tichelaar, B.W., Ruff, L.J., 1991. Seismic coupling along the Chilean subduction zone. J. Geophys. Res. 96, 11997–12022.
Valdes, C.M., Mooney, W.D., Singh, S.K., Meyer, R.P., Lomnitz, C., Luetgert, J.H., Helsley, C.E., Lewis, B.T.R., Mena, M., 1986. Crustal structure of Oaxaca, Mexico, from seismic refraction measurements. Bull. Seism. Soc. Am. 76, 547–563.
Váldes-Gonzalez, C., Meyer, R.P., 1996. Seismic structure between the Pacific coast and México City from Petatlan earthquake ($M_s = 7.6$) aftershocks. Geofis. Intern. 35, 377–401.